Received: 7 June 2019 | Revised: 12 August 2019 | Accepted: 15 September 2019

DOI: 10.1002/jbio.201900224

FULL ARTICLE

JOURNAL OF BIOPHOTONICS

Spectral characteristics of caries autofluorescence obtained from different locations and caries severities

Jung Hoon Ro[1] | John J. Bang[2] | Yong-Il Kim[3] | Dong-Joon Lee[4] | Ching-Chang Ko[5] | Franklin Garcia-Godoy[6] | Yong Hoon Kwon[7]*

[1]Department of Biomedical Engineering, School of Medicine, Pusan National University; Biomedical Research Institute, Pusan National University Hospital, Yangsan, South Korea

[2]Department of Environmental, Earth and Geospatial Sciences, North Carolina Central University, Durham, North Carolina

[3]Department of Orthodontics, School of Dentistry, Pusan National University, Yangsan, South Korea

[4]School of Dentistry, NC Oral Health Institute, University of North Carolina, Chapel Hill, North Carolina

[5]Department of Orthodontics, School of Dentistry, University of North Carolina, Chapel Hill, North Carolina

[6]Department of Bioscience Research, College of Dentistry, University of Tennessee Health Science Center, Memphis, Tennessee

[7]Department of Dental Materials, School of Dentistry, Pusan National University, Yangsan, South Korea

***Correspondence**
Yong Hoon Kwon, Department of Dental Materials, School of Dentistry, Pusan National University, Yangsan 50612, South Korea.
Email: y0k0916@pusan.ac.kr

Funding information
Pusan National University Hospital Biomedical Research Institute Grant, Grant/Award Number: 2017-B018

Abstract

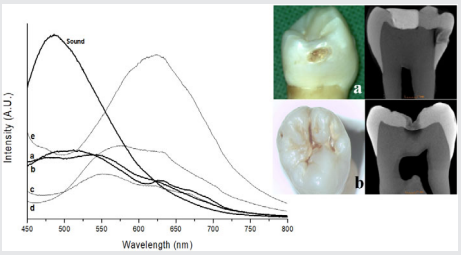

Dental caries usually occurs at interproximal and occlusal surfaces. The purpose of the present study was to determine if characteristic spectral factors extracted from autofluorescence (AF) spectra are informative regarding caries detection and the determination of caries stage as compared with DIAGNOdent results. AF spectra were obtained from caries lesions of different severities at two locations using a 405 nm laser. Three spectral factors, that is, spectral slope at 550 to 600 nm, spectral area under the curve at 500 to 590 nm and two-peak ratio between 625 and 667 nm, were extracted. The values of three spectral factors linearly decreased as caries progressed. According to micro-CT images, conventional visual and tactile inspections of lesions under or overestimated (25%-65%) caries states, and brown or thickly stained layer on interproximal or occlusal surfaces, respectively, caused misclassifications of caries stage. Of the spectral factors examined, spectral slope and area under curve for interproximal and occlusal surfaces, respectively, were found to be significantly related to caries stage and showed least data overlap. For interproximal and occlusal surfaces, DIAGNOdent readings of different stages overlapped considerably though their mean values were significantly different regardless of stage.

KEYWORDS

405 nm laser, caries diagnosis, DIAGNOdent, FTIR analysis, laser-induced autofluorescence, spectral analysis

1 | INTRODUCTION

Dental caries is one of the most common, chronic oral diseases and originates on tooth surfaces [1]. As a progressive and active disease, it can result in expensive restorations or extractions if it is not detected and treated properly. The condition is caused by acids produced by oral bacteria that reside everywhere on the tooth surface by forming a biofilm called plaque. They consume sugars and other carbohydrates and produce a range of acids [2–4]. These acids dissolve

minerals progressively from tooth surfaces, and thus, cause demineralization and cavity formation. Most dental plaque on smooth surfaces can be removed by daily brushing, but pits and grooves (occlusal surfaces) or regions between teeth (interproximal surface) are not easily cleaned due to the access difficulty of tooth brush, and thus, are highly susceptible to dental caries. In tooth cavities, minerals, such as calcium and phosphorous, lost by demineralization can usually be recharged by minerals dissolved in the saliva through a remineralization process [5–7], but this balance is altered when pH values on tooth surfaces fall below 4.3 and demineralization with subsequent browning and carious lesion decay accelerate [8].

An inspection of dental caries by tactile and visual inspections is a routine and primary process during dental visits. These processes are straightforward and conventional, but despite well-established guidelines, are heterogeneous and examiner dependent [9, 10]. An X-ray test can be added but the early detection of caries using this test is difficult. To improve the accuracy and efficiency of caries detection and diagnosis, several photonics-based adjunctive methods have been introduced, such as (digital image) fiber optic transillumination, quantitative light-induced fluorescence (QLF) and laser fluorescence (DIAGNOdent) with an aid of visual light or laser for excitation [11–13]. Alfano and Yao first reported on the phenomenon of autofluorescence (AF) almost 40 years ago, and since, it has been well investigated and used to develop medical devices that can detect caries [14]. Recently, a portable camera-type QLF device was available that uses 405 nm light as an excitation source to detect caries by fluorescence [15–17]. This technique can detect tooth surface changes, such as demineralization and the presence of porphyrins produced by oral bacteria. However, despite its many advantages, this device is bulky, and thus, its ability to detect occlusal or posterior lesions is limited by access issues. DIAGNOdent uses a 655 nm laser to produce AF [18, 19], and is nondestructive, easy to use and can detect caries in interproximal and occlusal surfaces. Nonetheless, despite claimed 70% to 80% sensitivities and specificities claimed for the detection of enamel and occlusal carious lesions, in vivo studies have produced conflicting results [20, 21].

For decades, fluorescence-based caries detection was carried out using lasers of various wavelengths ranging from the UV to visible red [22–24]. Since AF is produced as a result of light-chromophore interactions, it depends on excitation wavelength and the nature of the chromophore. However, chromophores on teeth include inorganic minerals and porphyrins, which can interact with light independently or in combination in a wavelength-dependent manner, which complicates interpretations of emission spectra. The advent of laser-diode technology resulted in the recent development of an inexpensive 405 nm light source, which has been well used for scientific researches. In particular, in the dental field, this 405 nm laser has been used as an excitation source for caries detection [25–27]. The advantage of this wavelength over others for caries detection is that the light can interact both with inorganic minerals and porphyrins. According to studies performed on the topic, AF spectra of sound teeth show an emission peak near 487 to 500 nm followed by a gradually decreasing emission profile near 800 nm. On the other hand, as caries progresses, spectral distributions change, for example, the intensities of some peaks reduce and new peaks appear. However, the majority of studies conducted to date have been focused on detection of caries or sought to confirm the ability of the 405 nm laser to detect caries, and few have addressed the ability of this laser to assess caries severity by stage and comparison with DIAGNOdent, another caries detection device.

Interproximal and occlusal surfaces have obviously different morphologies, as interproximal surfaces have round, smooth surfaces, whereas occlusal surfaces have bumps and trench-like grooves. Furthermore, location and morphology differences can affect bacterial habitation, plaque formation and the severity of demineralization. As a result, such differences may affect the composition and structure of lesions and the severity of caries, and thus, affect resultant AF spectra, which suggests spectra produced by caries of different severities at interproximal and occlusal surfaces might have different spectral characteristics. Therefore, the purpose of the present study was to identify spectral factors useful for quantifying caries severity. To achieve this, the characteristic spectral factors were extracted from the AF spectra of caries lesions at interproximal and occlusal surfaces using a 405 nm laser as an excitation source. These factors were compared with each other and with DIAGNOdent readings. In addition, these data were compared with Fourier-transform infrared spectroscopy (FTIR) and other imaging findings with respect to lesion locations and severities.

2 | MATERIALS AND METHODS

2.1 | Tooth preparation and caries staging

For the study, the teeth (315 molars and premolars) were cleaned, frozen and stored at 100% relative humidity after extraction. The Institutional Review Board at Pusan National University Dental Hospital (Yangsan, Republic of Korea) approved the study protocol and waived the requirement for informed consent. Two examiners inspected the teeth independently by eye, optical microscopy and by tactile inspection using an explorer. Teeth were classified as sound, stage II, III or IV (Table 1) based on caries severity; teeth were classified in an identical manner by the two examiners.

TABLE 1 Description of caries stages defined in this study

	Description	
Code	**Interproximal surface**	**Occlusal surface**
Sound	Sound and glossy surface	No visible stain and carious lesion
Stage II	Demineralization less 1/3 enamel, visible white spot, no glossy surface, remineralization can occur, dentist warns finding of incipient caries	Visible light brown stain but no visible carious lesion, or minor demineralization around pit & fissure; dentists recommend careful brushing and prevent fluoride treatment
Stage III	Demineralization over 1/3 enamel and possibly damaged to dentin, more clearly visible white spot than stage II, sometimes light to dark brown spot is visible, no cavitation yet, immediate treatment depend on internal demineralization	Visible dark brown stain with, sometimes, noncavitated white chalky enamel on pit & fissure; recommend treatment
Stage IV	Cavitation is visible and progressed into dentin, white and/or brown discolored lesion is frequently visible, immediate treatment is required	Visible stain with cavitated lesion; immediate treatment is required
Code	**Relevant ADA Caries Classification**	**Relevant ICDAS II**
Sound	Sound (No clinical detectable lesion)	Sound tooth surface (0)
Stage II	Initial (Earliest clinically detectable lesion compatible with mild demineralization)	First/Distinct visual change in enamel (1,2)
Stage III	Moderate (Enamel breakdown, moderate dentin demineralization)	Enamel breakdown, no dentin visible (3)
Stage IV	Advanced (Full enamel cavitation and dentin exposure. Dentin lesion is deeply and severely demineralized)	Underlying dentinal shadow (not cavitated into dentin)—in our case, this case was grouped to III if there is no loss of surface integrity (4) Distinct cavity with visible dentin (5) Extensive distinct cavity with visible dentin (6)

Abbreviations: ADA, American Dental Association; ICDAS, International Caries Detection and Assessment System.

Twenty teeth from each stage were then randomly selected and these 80 teeth constituted the study groups. Subsequently, teeth were re-examined by micro-CT (inspeXio SMX-90CT, Shimadzu, Tokyo, Japan) at 90 kV and 100 μA, because this technique allowed nondestructive visualization of lesions from enamel surface to dentin subsurface.

2.2 | Autofluorescence analysis

The laser-induced AF spectra of teeth were obtained using a 405 nm laser (LVI Technology, Seoul) at an output power of 2 ± 0.1 mW, as determined using a power meter (PM3/FieldMax, Coherent, Portland, Oregon). To achieve stable, minimally fluctuating output power, the original power (100 mW) was attenuated by 98% using various combinations of filters (Thorlabs, Inc, Newton, New Jersey). Each tooth was then placed on an XYZ-stage to ensure consistent positioning. The laser was normally focused on the center of each lesion using a convex lens ($f = 10$ cm) for 1 s. Emission spectra were recorded using a spectrometer (QE65000FL, Ocean Optics, Inc, Dunedin, Florida) by guiding emitted light through an optical fiber (QP600-1-UV-VIS; 600 μm diameter silica core), which was aligned at 35° to 45° with respect to the direction of the laser beam. The detection range of the spectrometer was 200 to 1100 nm and its optical resolution (grating #: 300; slit size: 200 μm) was 6.5 nm. The end of the optical fiber (detector) was

positioned 1 cm away from lesion surfaces, and a 450 nm longpass filter (Thorlabs, Inc) was placed in front of the optical fiber to attenuate the incident light.

To determine caries stages from AF spectra, three factors were extracted and assessed, that is, spectrum slope at 550 to 600 nm, spectral area under the curve at 500 to 590 nm and two-peak ratio. Spectral area under the curve at 500 to 590 nm was determined by integrating the curve using ORIGIN (Microcal Software, Inc, Southampton, Massachusetts). Two-peak ratio (625/667 nm) was calculated by dividing the peak intensity at 625 nm by that of at 667 nm.

2.3 | DIAGNOdent test

Carious lesions in specimens were tested using a DIAGNOdent pen (KaVo Dental, Biberach, Germany), according to the manufacturer's instructions. Before measurements, the device was calibrated against a ceramic standard. Three measurements were taken per lesion by moving the pen slightly. Peak digital values were classified as follows: 0 to 13, healthy; 14 to 20, beginning of demineralization; 21 to 29, strong demineralization; and >30, dentin caries, as described by the manufacturer. Values of >30 indicate the consideration of an X-ray test and a possible minimally invasive treatment or resin filling. The manufacturer's guidelines do not match the description given in Table 1 precisely, but healthy (0–13), beginning demineralization (14–20), strong demineralization (21–29) and dentin caries (>30) corresponded approximately to sound, stage II, stage III and stage III/IV, respectively, according to our classification.

2.4 | Micro-CT images

To obtain computerized tomography (CT) images of specimens with caries at different stages, micro-CT (inspeXio SMX-90CT, Shimadzu, Tokyo, Japan) was used at 90 kV and 100 μA and a slice width of 1 mm. Specimens were sectioned both longitudinally and transversely.

2.5 | Fourier-transform infrared spectroscopy

To analyze compositional changes in carious lesions, a FTIR spectrophotometer (Nicolet 6700/8700, Thermo Fisher Scientific, Inc, Waltham, Massachusetts) connected to an attenuated total reflection accessory was used to obtain spectra in the range 7800 to 350 cm^{-1}. Each specimen was scanned 32 times at a resolution of 0.09 cm^{-1}. In addition, 2 mg of ground powder was obtained from each lesion using a fissure bur and then mixed with 10 mg of potassium bromide and subjected to thin film FTIR.

2.6 | Statistical analysis

The results (spectrum slopes at 550–600 nm, spectral areas under the curve at 500–590 nm, 625 vs 667 nm two-peak ratios and DIAGNOdent readings) were analyzed by one-way ANOVA followed by Tukey's post hoc test for multiple comparisons. The student's *t* test was performed to compare interproximal and occlusal surface results. *P* values of <.05 were considered significant throughout.

3 | RESULTS

Table 2 lists the number of specimens allocated to sound, and stages II, III and IV after visual and tactile inspections, and again after micro-CT analysis for interproximal and occlusal surfaces. Of the 20 specimens chosen per stage, 13, 15 and 12 (for interproximal surfaces) and 7, 10 and 14 (for occlusal surfaces) were reclassified as stages II, III and IV, respectively, after micro-CT analysis. Visual and tactile inspections misclassified (over or underestimated) caries by 25% to 40% and 30% to 65% for interproximal and occlusal surfaces, respectively, depending on the stage (severity).

Figure 1 shows optical microscope (a, c, e) and micro-CT (b, d, f) images of stage IV carious lesions on interproximal and occlusal surfaces. Under the microscope, only the

TABLE 2 The number of specimens after visual and tactile inspections and the number of reclassified specimens based on the micro-CT analysis using the same specimens used for visual and tactile inspections

	Number of specimens		
		After micro-CT analysis which were visually and tactilely inspected	
	After visual and tactile inspection	Interproximal surface	Occlusal surface
Sound	20	Sound: 20	Sound: 8, Stage II: 10, Stage III: 2
Stage II	20	Sound: 2, Stage II: 13, Stage III: 5	Sound: 7, Stage II: 7, Stage III: 6
Stage III	20	Stage II: 2, Stage III: 15, Stage IV: 3	Stage II: 10, Stage III: 10
Stage IV	20	Stage III: 8, Stage IV: 12	Stage III: 6, Stage IV: 14

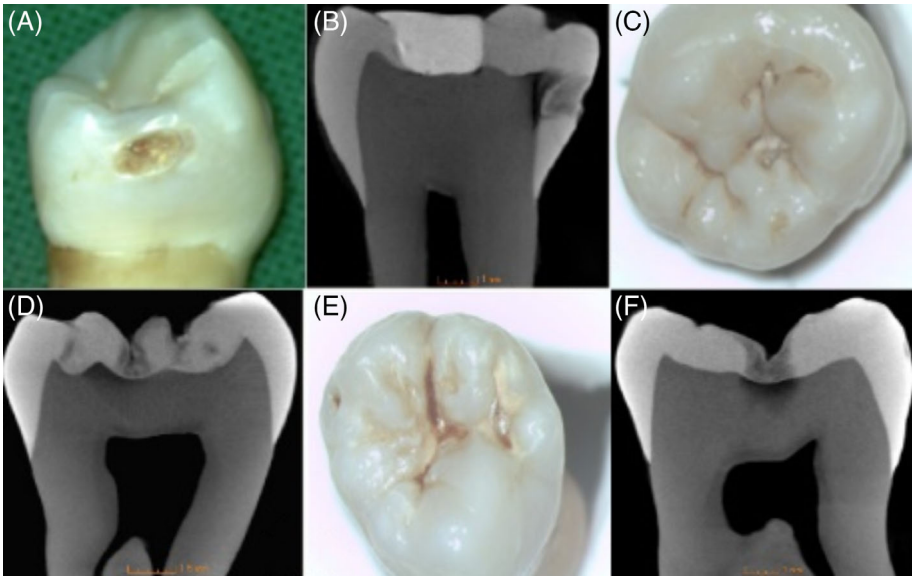

FIGURE 1 Optical microscope (a, c, e) and micro-CT (b, d, f) images of stage IV lesions on interproximal and occlusal surfaces. Specimen e had a dark brown stain with a thick layer on a groove. Image f is a micro-CT image of specimen e

margins, colors and severities of lesions on surfaces were observable, whereas micro-CT images depicted lesion depth and width regardless of the tooth condition.

Figure 2 shows one representative AF spectrum of specimens with caries affecting interproximal and occlusal surfaces and different caries stages (a, b). Spectra showed sharply or mildly increasing toward the emission peak at 485 to 490 nm and then gradually diminishing to baseline

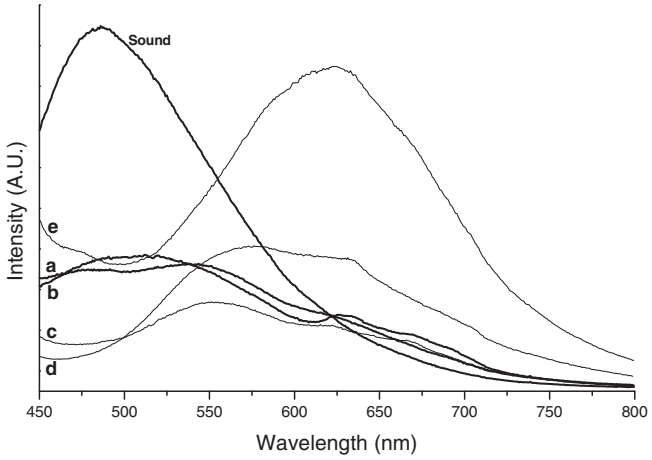

FIGURE 2 Representative autofluorescence (AF) spectra obtained from different specimen surfaces (interproximal and occlusal surfaces) for sound and stage IV caries (sound, a, b). Two AF spectra for stage IV were similar despite locational difference. Fluorescence maxima in the region of 630 to 700 nm could be addressed to endogenous porphyrins and/or layer of calculus. Usually caries lesions had a brown stain on interproximal surfaces or sometimes a thick layer on grooves. Some specimens had spectral slopes at 450 to 500 and after 500 nm that differed from a and b though visually they had similar discolorations on interproximal surfaces (c). Spectral distributions of stained thick layers on grooves (d) and ground powder (e) of this layer were similar

with different slopes as caries progressed from sound to stage IV. AF spectra from interproximal and occlusal surfaces were similar. As caries progressed, brown staining was commonly observed in caries lesions. Basically, specimens exhibited similar AF patterns, but even specimens of the same stage had slightly different spectral profiles, slopes and areas under the curve. Some AF spectra (c, d) showed a decrease and then an increasing profile at 450 to 500 nm and then increasing profile with one or two emission peak(s) after 500 nm. In addition, some specimens with a thick stained layer on a groove had spectral profiles (d, e) that differed from representative AF spectra. However, when this layer was slightly removed by polishing spectral profiles more resembled representative spectra.

Tables 3 and 4 show the means, standard deviation, and minimum and maximum values of the three factors (spectrum slope at 550-600 nm, spectral area under the curve at 500-590 nm and two-peak ratio between 625 and 667 nm) and the DIAGNOdent results of interproximal and occlusal surface specimens and statistical analysis. On interproximal surfaces, spectrum slopes and DIAGNOdent readings of caries stages differed significantly ($P < .001$). On the other hand, the spectral curve areas and DIGNOdent readings for occlusal surface were found to be significantly different depending on caries stage ($P < .001$). For some factors, stages II and III were similar regardless of location. According to t test, spectrum slope was significantly different for two surfaces and caries stages, except sound teeth ($P < .05$). In most cases, however, spectral area and peak ratio were not significantly different regardless of caries stage or location.

Figures 3 and 4 show scatter plots (Table 3) of the three factors. For interproximal surfaces (Figure 3), spectral slope at 550 to 600 nm showed least overlap between caries stages

TABLE 3 The estimated values from the AF spectrum and DIAGNOdent readings for specimens of different caries stages which were reclassified based on the micro-CT analysis

	Interproximal surface				
	Sound[a]	**Stage II[b]**	**Stage III[c]**	**Stage IV[d]**	***P*-value**
Slope at 550-600 nm	74.9 ± 9.8	45.6 ± 7.5	33.3 ± 2.7	20.2 ± 7.8	<.001
	(58.6-98.7)	(31.2-54.1)	(28.7-37.0)	(4.3-30.1)	
	Sound[a]	Stage II[b]	Stage III[b]	Stage IV[c]	
Spectral area under at 500-590 nm	883.3 ± 80.9	656.1 ± 66.1	627.8 ± 74.6	470.1 ± 61.4	<.001
	(753-1076)	(545-743)	(553-783)	(328-553)	
	Sound[a]	Stage II[b]	Stage III[b]	Stage IV[c]	
Ratio between 625/667 nm	1.31 ± 0.03	1.22 ± 0.04	1.19 ± 0.06	1.13 ± 0.08	<.001
	(1.26-1.37)	(1.14-1.27)	(1.05-1.31)	(0.95-1.20)	
	Sound[a]	Stage II[b]	Stage III[c]	Stage IV[d]	
DIAGNOdent reading	8.6 ± 2.0	35.5 ± 14.3	77.7 ± 17.0	96.2 ± 5.5	< 0.001
	(5.3-12.7)	(12.3-60.7)	(40.7-96.7)	(83.0-99.0)	
	Occlusal surface				
	Sound[a]	**Stage II[b]**	**Stage III[b]**	**Stage IV[c]**	***P*-value**
Slope at 550-600 nm	73.4 ± 7.5	30.5 ± 10.0	23.7 ± 5.8	12.6 ± 5.4	<.001
	(60.1-81.8)	(19.4-45.9)	(16.7-32.9)	(4.7-23.4)	
	Sound[a]	Stage II[b]	Stage III[c]	Stage IV[d]	
Spectral area under at 500-590 nm	942.0 ± 91.9	630.3 ± 60.5	528.0 ± 36.7	391.2 ± 63.6	<.001
	(811-1088)	(580-727)	(471-580)	(287-484)	
	Sound[a]	Stage II[b]	Stage III[b]	Stage IV[c]	
Ratio between 625/667 nm	1.32 ± 0.05	1.22 ± 0.03	1.21 ± 0.03	1.11 ± 0.05	<.001
	(1.25-1.38)	(1.19-1.27)	(1.16-1.26)	(0.96-1.17)	
	Sound[a]	Stage II[b]	Stage III[c]	Stage IV[d]	
DIAGNOdent reading	32.2 ± 9.1	43.8 ± 17.5	69.6 ± 19.5	96.0 ± 4.8	<.001
	(21.0-47.3)	(25.0-70.7)	(47.5-99.0)	(85.0-99.0)	

Note: Statistically significant difference on carious stage is shown by superscript letters[a, b,…]. Same letters in the same row are not significantly different ($P > .05$).
Abbreviation: AF, autofluorescence.

TABLE 4 Results of the *t* test between interproximal and occlusal surfaces for different caries stages and factors

	Sound	**Stage II**	**Stage III**	**Stage IV**
Slope at 550-600 nm	NSD	SD	SD	SD
Spectral area under at 500-590 nm	NSD	NSD	SD	SD
Ratio between 625/667 nm	NSD	NSD	NSD	NSD
DIAGNOdent reading	SD	NSD	NSD	NSD

Note: NSD, not significantly different; SD, significantly different.

than the other two factors. On the other hand, for occlusal surfaces (Figure 4), area under the curve at 500 to 590 nm showed least overlap. For DIAGNOdent readings, despite significantly different mean values for each stage, results showed considerable overlap between stages for interproximal and occlusal surfaces.

Figure 5 shows representative FTIR spectra of sound interproximal and occlusal surfaces. Figure 6 shows spectra of sound, stage IV specimen without any apparent thickly stained brown layer on groove, and powder of the ground-stained layer. Except the ground powder, no apparent compositional changes that reflect locational variation or caries severities were observed. Assigned characteristic bands were CO_3^{2-} (1550, 1460–1415 and 870 cm^{-1}), PO_4^{3-} (1090–1032 and 960 cm^{-1}), C—H (2930 and 2860 cm^{-1}) and water/OH^- (3700–3400 cm^{-1}). However, some occlusal specimens had

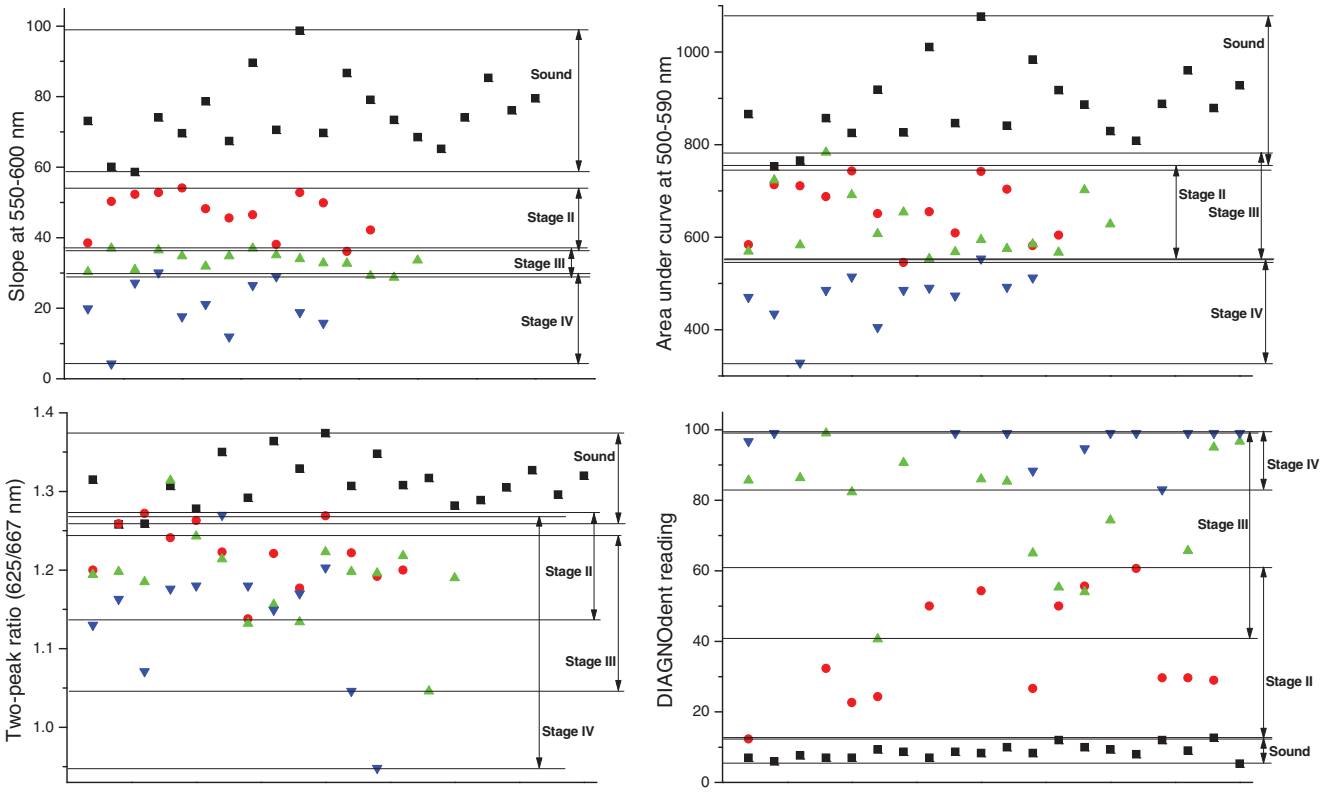

FIGURE 3 Scatter plots of data obtained from interproximal surfaces. Of the three spectral factors, slope at 550 to 600 nm shows least data overlap between stages. In the case of DIAGNOdent results, stage III showed considerable overlap with stages II and IV, though their mean values are significantly different regardless of caries stage

a dark, thick, brown stain on grooves (Figure 1e). The powder obtained from that thickly stained layers showed amide bands at 1250 (amide III), 1548 (amide II) and 1668 cm^{-1} (amide I), which were assigned to amino acids (Figure 6).

4 | DISCUSSION

The detection of caries is important to maintain healthy teeth, and the diagnosis of the caries stage based on severity is essential for proper and timely treatment. Caries is usually detected and diagnosed during visits to dental clinics made for regular check-ups [11, 12], and is routinely and straightforwardly diagnosed by visual and tactile inspections. This method provides a simple, first approach, but is subjective despite the presence of classification guidelines, such as the American Dental Association (ADA) Caries Classification or International Caries Detection and Assessment System (ICDAS). This method is useful only for surface observations and sometimes causes inaccurate judgment if the examiner is inexperienced, and an X-ray is required when a lesion is suspicious. X-ray is superior to visual and tactile inspection because it provides detail of internal tooth structure, but X-ray testing is insensitive for early and mild caries, and is not recommended for the diagnosis of these stages.

In the present study, a simplified 4-stage classification, which is similar to ADA and ICDAS classification guidelines, was used because this classification seems suitable for decision making regarding whether to observe further or treat a suspicious lesion immediately when a patient is present. In the present study, such decisions were made using AF spectra. Furthermore, tests like those used in the present study could be useful for determining the feasibility of using our 4-stage classification based on AF spectroscopy in conjunction with a 405 nm laser. Actually, the present method, based on the AF spectrum and spectral analysis, would be useful for critical stages, such as stage II or III, so the practice can be less risky. In the present study, the findings of visual and tactile inspections matched those of micro-CT images 35% to 75% depending on stage. Low matches for occlusal surfaces for stages II and III (7/20 and 10/20, respectively; for interproximal surfaces corresponding matches were 13/20 and 15/20, respectively) were attributed to an irregular, grooved morphology in the absence of visible cavitation. In addition, white spots or dark brown stained lesions may have led to incorrect caries staging [28–30]. In the case of interproximal surfaces, 2/5(=7), 2/3(=5) and 8/0 (=8) of 20 stages II, III and IV (Table 2) specimens, respectively, were over/underestimated due to the presence of a

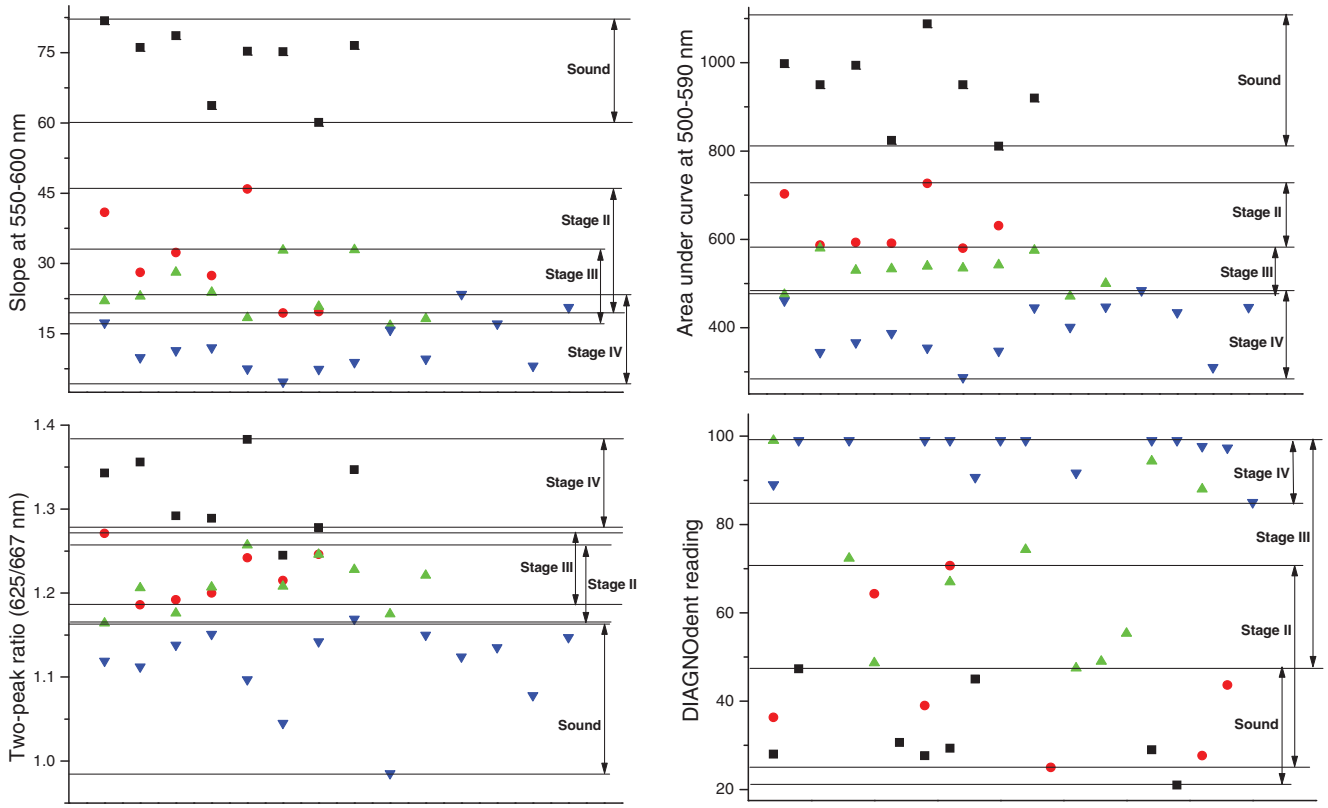

FIGURE 4 Scatter plots of data obtained from occlusal surfaces. Of the three spectral factors, area under curve at 500 to 590 nm showed least data overlap between stages. DIAGNOdent results for sound teeth showed considerable overlap with stages II and III results and stages II and IV results also showed much overlap

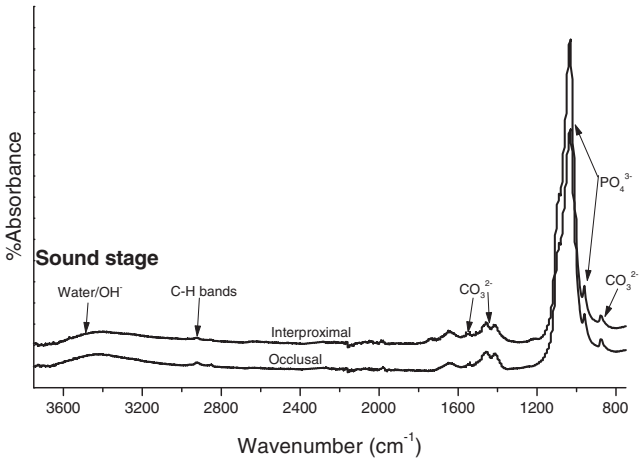

FIGURE 5 Representative Fourier-transform infrared spectra obtained from interproximal and occlusal surfaces of two sound teeth. Despite locational differences, two surfaces had the same compositions

dark brown stain on lesions. Also, for occlusal surfaces, 7 of 14 stage IV specimens had a thick layer of dark brown stain on a groove. However, this thick layer was not often observed in stage III.

Laser-induced AF is the result of a laser-chromophore interactions within the tissue. The representative AF spectrum of sound teeth obtained using the 405 nm laser showed a characteristic spectral distribution from 450 to 800 nm with an emission peak near 485 to 490 nm and a baseline close to 800 nm owing to both inorganic and organic substances [31–33]. The principal constituent, carbonated hydroxyapatite produces AF in the 450 to 600 nm region. As caries progresses, peak intensity at 485 to 490 nm and spectral slope in this region decreased gradually, and spectral area under the curve at 500 to 590 nm also diminished. In the oral cavity, caries occurs as a result of tooth demineralization by the acids formed by bacteria, such as *Streptococcus mutans* and *Lactobacillus*, which produce acetic, lactic or propionic acids as byproducts of carbohydrate consumption [2, 3]. Minerals in saliva can replace dissolved minerals, but when the rate of demineralization exceeds that of remineralization, caries progresses with subsequent loss of tooth morphology. Decay of a weakened tooth surface is promoted by external stresses, such as mastication-associated forces, and gradually a cavity forms with a covering dark brown stain. Since demineralization-remineralization is a long-term dynamic process, discoloration by, for example, foods and drinks, smoking, tartar and poor oral hygiene, is highly probable. A dark brown stain in these lesions can absorb

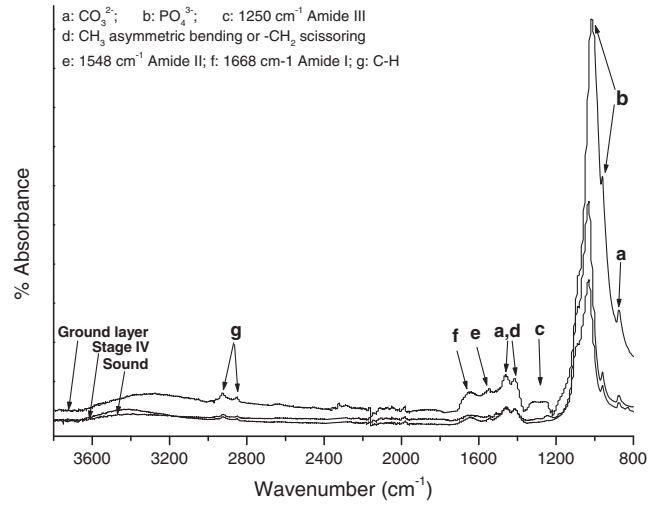

FIGURE 6 Representative Fourier-transform infrared spectra obtained from the occlusal surfaces of sound and stage IV teeth and of powdered layer. The powder was obtained by grinding the dark brown stained layer. The spectrum of ground layer differed from those of sound and stage IV specimens and this difference was attributed to the presence of amino acids (c, e, f: amide groups)

much incident light and the irregular porous structure of lesions increase light scattering, which means AF intensities are reduced [34]. Dental calculus or any undetermined fluorescent component in foods or drinks that cause brown stains may produce additional peaks after 600 nm [35, 36]. Also, oral bacteria and endogenous porphyrins (e.g., protoporphyrin IX) synthesized by oral bacteria in the carious lesions [31–33] produce one or two narrow weak or wide strong peaks after 600 nm. However, the diversity of biofilms on teeth, dietary habits, personal habits and tooth brushing frequencies, may unpredictably and complicatedly affect brown stain intensities and the concentrations and types of oral bacteria and endogenous porphyrins on lesions. The causes of abnormalities in spectral profiles in the 450 to 500 nm and after 500 nm regions are not clear, but, they may be complicatedly related with tartar, demineralization (or infrequently from diabetic patients, due to pregnancy, etc) in addition to oral bacteria and endogenous porphyrins related to non or carious lesions and conditions of the teeth.

In the present study, not all brown-stained specimens had the same AF spectrum, and thus, specimens with abnormal AF profiles in these ranges were treated as outliers and excluded from the reclassification, though their caries stages were correctly determined by micro-CT analysis. The excluded specimens had decrease and then increasing AF profiles at 450 to 500 nm and one or two wide peak(s) after 500 nm. These are different AF patterns compared to those of normal representative AF patterns.

Three characteristic factors are useful for the diagnosis of caries stage can be extracted from AF spectra [25] based on caries severity associated changes in spectral patterns. Spectral slope at 550 to 600 nm is one such factor. This region was chosen based on the observation that most specimens tested showed a strong inverse linear correlation (close to 1) between AF intensity and emission wavelength. The second factor is spectral area under the curve at 500 to 590 nm. As caries progresses, the spectral area under the curve at 500 to 590 nm has reduced due to the decreased emission intensity. The third factor is a peak ratio between 625 and 667 nm emission intensities. Sometimes, one or two peaks attributable to oral bacteria, endogenous porphyrins or dental calculus are also observed at these wavelengths. In interproximal and occlusal surfaces, spectral slope, spectral area and two-peak ratio were in the ranges, 12.6 to 74.9, 391.2 to 942.0 and 1.11 to 1.32, respectively, and all three factors showed similar linearly decreasing trends as caries stage increased. On the other hand, this decrease was much faster for occlusal surfaces. In fact, spectral slope, spectral area under the curve, and two-peak ratio were found to correlate linearly with caries stage ($R > .92$) regardless of lesion location. In addition, the three factors showed a strong linear correlation ($R > .98$) with each other on interproximal and occlusal surfaces. DIAGNOdent readings increased linearly as caries progressed. For sound and stage II cases, values of occlusal surfaces were greater than those of interproximal surfaces. In addition, for both interproximal and occlusal surfaces, three factors showed an inverse linear correlation with DIAGNOdent readings in the range 0.85 to 0.96.

Some occlusal specimens of stage III or IV showed dark brown staining with a thick layer on grooves. The spectral distributions of these specimens were similar to those of ground powder samples of these layers, but differed from those of stage IV interproximal or occlusal surfaces, which had no stained layer. On the other hand, when these layers were removed by grinding, spectral distributions became similar to those of representative AF spectra of interproximal or occlusal surfaces of stage IV (not shown in Figure 2). According to FTIR analysis, the principal compositions of lesions were not altered by caries progression, except for a minor decrease in intensity due to demineralization. On the other hand, the powder collected from grooves showed peaks attributable to amide and C─H bonds [37]. It can be suggested that amino acids had accumulated at the bottom of grooved occlusal surface as a sediment, which then hardened. These hardened layers are not removed easily by normal brushing owing to the irregular, grooved surface morphology, which is one of the reasons why these hardened layers are found more frequently on occlusal surfaces. Furthermore, because these layers

produce different spectral patterns, they can result in incorrect staging when an examiner is inexperienced. In the present study, some specimens with normal micro-CT images were spectroscopically exceptional due to the presence of brown staining on the interproximal surface or thickly stained brown layer on occlusal surfaces. Exceptional AF spectra from the lesions are probably attributable to any unidentified fluorescing component in foods and drinks, tartar or endogenous porphyrins. These components can be included as a mixture of diverse combinations and then remain in the stain or a layer owing to incomplete removal of them or as a sediment.

5 | CONCLUSION

According to micro-CT analysis, 25% to 40% and 30% to 65% of interproximal and occlusal surface specimens, respectively, evaluated by visual and tactile inspection were misclassified. Brown stain or a thickly stained brown layer on carious lesions caused misclassification of caries stage and sometimes produced abnormal AF spectra in the 450 to 500 nm and after 500 nm ranges. Of the spectral factors tested, spectral slope at 550 to 600 nm and spectral area under the curve at 500 to 590 nm showed consistent and significantly different mean values for each caries stage and least overlap between caries stages as determined by a scatter plot. In the case of DIAGNOdent, mean values for each stage on both interproximal and occlusal surfaces were significantly different, but data showed much overlap between stages for both surfaces. AF spectra obtained from interproximal and occlusal surfaces showed similar spectral profiles despite locational differences.

ACKNOWLEDGMENT

This study was supported by Biomedical Research Institute Grant (2017-B018), Pusan National University Hospital.

CONFLICTS OF INTEREST

None of the authors have any conflicts of interest.

ORCID

Yong Hoon Kwon https://orcid.org/0000-0001-8097-2114

REFERENCES

[1] R. H. Selwitz, A. I. Ismail, N. B. Pitts, *Lancet* **2007**, *369*, 51.
[2] W. J. Loesche, *Microbiol. Rev.* **1986**, *50*, 353.
[3] F. O. van Ruyven, P. Lingström, J. van Houte, R. Kent, *J. Dent. Res.* **2000**, *79*, 778.
[4] N. Takahashi, B. Nyvad, *J. Dent. Res.* **2011**, *90*, 294.
[5] R. J. Lynch, R. Navada, R. Walia, *Int. Dent. J.* **2004**, *54*, 304.
[6] N. J. Cochrane, F. Cai, N. L. Huq, M. F. Burrow, E. C. Reynolds, *J. Dent. Res.* **2010**, *89*, 1187.
[7] D. Cummins, *J. Dent.* **2013**, *41*, S1.
[8] H. C. Margolis, Y. P. Zhang, C. Y. Lee, R. L. Kent Jr. , E. C. Moreno, *J. Dent. Res.* **1999**, *78*, 1326.
[9] T. Gimenez, C. Piovesan, M. M. Braga, D. P. Raggio, C. Deery, D. N. Ricketts, K. R. Ekstrand, F. M. Mendes, *J. Dent. Res.* **2015**, *94*, 895.
[10] S. Twetman, *J. Evid. Based Dent. Pract.* **2015**, *15*, 182.
[11] I. A. Pretty, R. P. Ellwood, *J. Dent.* **2013**, *41*, S12.
[12] S. Twetman, S. Axelsson, G. Dahlén, I. Espelid, I. Mejàre, A. Norlund, S. Tranæus, *Acta Odontol. Scand.* **2013**, *71*, 388.
[13] E. de Josselin de Jong, F. Sundström, H. Westerling, S. Tranaeus, J. J. ten Bosch, B. Angmar-Månsson, *Caries Res.* **1995**, *29*, 2.
[14] R. R. Alfano, S. S. Yao, *J. Dent. Res.* **1981**, *60*, 120.
[15] H. E. Kim, B. I. Kim, *Photodiagnosis Photodyn. Ther.* **2018**, *23*, 45.
[16] H. S. Lee, S. K. Kim, S. W. Park, E. de Josselin de Jong, H. K. Kwon, S. H. Jeong, B. I. Kim, *J. Biomed. Opt.* **2018**, *23*, 1.
[17] A. M. Maria, A. Z. de Freitas, S. L. de Campello, A. S. Gomes, L. Karlsson, *J. Biophotonics* **2016**, *9*, 596.
[18] M. M. Braga, F. Mendes, K. R. Ekstrand, *Dent. Clin. N. Am.* **2010**, *54*, 479.
[19] T. Gimenez, M. M. Braga, D. P. Raggio, C. Deery, D. N. Ricketts, F. M. Mendes, *PLoS One* **2013**, *8*, e60421.
[20] X. Q. Shi, U. Welander, B. Angmar-Månsson, *Caries Res.* **2000**, *34*, 151.
[21] A. Reis, F. M. Mendes, V. Angnes, G. Angnes, R. H. Grande, A. D. Loguercio, *J. Dent.* **2006**, *34*, 89.
[22] F. Sundstrom, K. Fredriksson, S. Montan, U. Hafstrom-Bjorkman, J. Strom, *Swed. Dent. J.* **1985**, *9*, 71.
[23] A. F. Hall, E. DeSchepper, M. Ando, K. Stookey, *Adv. Dent. Res.* **1997**, *11*, 507.
[24] E. Borisova, T. Uzunov, L. Avramov, *Lasers Surg. Med.* **2004**, *34*, 249.
[25] C. C. Ko, D. H. Yi, D. J. Lee, J. Kwon, F. Garcia-Godoy, Y. H. Kwon, *J. Dent.* **2017**, *67*, 77.
[26] J. C. Simon, K. H. Chan, C. L. Darling, D. Fried, *Lasers Surg. Med.* **2014**, *46*, 203.
[27] L. Zhang, A. S. Kim, J. S. Ridge, L. Y. Nelson, J. H. Berg, E. J. Seibel, *J. Biomed. Opt.* **2013**, *18*, 111412.
[28] A. Ribeiro, C. Rousseau, J. Girkin, A. Hall, R. Strang, C. John Whitters, S. Creanor, A. S. Gomes, *J. Dent.* **2005**, *33*, 73.
[29] D. F. Côrtes, R. P. Ellwood, K. R. Ekstrand, *Caries Res.* **2003**, *37*, 8.
[30] C. Robinson, R. C. Shore, S. J. Brookes, S. Strafford, S. R. Wood, J. Kirkham, *Crit. Rev. Oral Biol. Med.* **2000**, *11*, 481.
[31] S. Lu, F. Pereira, S. E. Fraser, M. Gharib, *J. Biomed. Opt.* **2008**, *13*, 024014.
[32] W. Buchalla, A. M. Lennon, T. Attin, *Eur. J. Oral Sci.* **2004**, *112*, 490.
[33] C. M. Volgenant, M. H. van der Veen, J. J. de Soet, J. M. ten Cate, *J. Oral Sci.* **2013**, *121*, 156.

[34] I. A. Pretty, W. M. Edgar, S. M. Higham, *Arch. Oral Biol.* **2004**, *49*, 285.
[35] W. Buchalla, A. M. Lennon, T. Attin, *J. Periodontal Res.* **2004**, *39*, 327.
[36] S. P. Singh, P. Falt, I. Barman, A. Koistinen, R. R. Dasari, A. M. Kullaa, *J. Biophotonics* **2017**, *10*, 1279.
[37] P. Seredin, V. Kashkarov, A. Lukin, Y. Ippolitov, R. Julianc, S. Doyle, *J. Synchrotron Rad.* **2013**, *20*, 705.

How to cite this article: Ro JH, Bang JJ, Kim Y-I, et al. Spectral characteristics of caries autofluorescence obtained from different locations and caries severities. *J. Biophotonics*. 2019; e201900224. https://doi.org/10.1002/jbio.201900224